(RE)ACTIONS OF THE EARTH SYSTEM: correlation analysis in a regime of passive stability of the surroundings

Ingryd Frederico Oliveira
Student, Escola Estadual de Ensino em Tempo Integral Professor Alejandro Yague Mayor
Avenida Aracajú, 3780, Jorge Teixeira, 76912-645, Ji-Paraná/RO
570212@aluno.seduc.ro.gov.br

Cauan Barros Da Rocha
Student, Escola Estadual de Ensino em Tempo Integral Professor Alejandro Yague Mayor
Avenida Aracajú, 3780, Jorge Teixeira, 76912-645, Ji-Paraná/RO
569975@aluno.seduc.ro.gov.br

Sidnei Pereira Oliveira
Teacher, Escola Estadual de Ensino em Tempo Integral Professor Alejandro Yague Mayor
Avenida Aracajú, 3780, Jorge Teixeira, 76912-645, Ji-Paraná/RO
sidneiunir@seduc.ro.gov.br

ABSTRACT

Ji-Paraná (RO) faces a dengue alert with the reintroduction of DENV-3, highlighting the need for simple local metrics. We investigated the correlation between temperature and precipitation with larval infestation (Mosquito Habitat Mapper - MHM protocol) and atmospheric series (INMET, NASA). In nine neighborhoods, we monitored weekly for five weeks (07/09–11/10/2025). We detected 86 larvae, with a peak in Week 3 (29 larvae) under 37.20 mm of rain. There was a moderate positive association between rain and larvae ($r = 0.52$) and a moderate negative association between average temperature and larvae ($r = -0.63$), indicating an optimal thermal window for the vector/virus. We conclude that MHM + INMET/NASA is viable as a local weekly indicator for post-rain blockades, risk communication, and educational actions. We recommend extending the series, increasing the sample size, testing for lags, and modeling nonlinearities. The mentorship was crucial for the quality and scalability of the model.

KEYWORDS. Dengue. Citizen science. Mosquito Habitat Mapper, GLOBE Program. Predictive surveillance.

1. Research Question and Problem Statement

In 2025, Ji-Paraná (RO) faces a scenario of increased risk for dengue, with an alert for the reintroduction of the dengue virus serotype 3 (DENV-3) and reports of high Aedes aegypti infestation across various neighborhoods. This situation pressures public health surveillance and demands strategies that go beyond the reactive model (Nogueira, 2025; Pessoa, 2025b). Recent local evidence indicates heterogeneous incidence among different areas of the city and highlights the need for simple, actionable metrics for territorial prioritization (Goulart *et al.*, 2024). Historically, Rondônia has recorded increases in cases and associated social costs, reinforcing the urgency for evidence-based solutions (Abe & Miraglia, 2018).

The literature demonstrates that temperature and precipitation influence the eco-epidemiology of dengue, allowing for risk anticipation when analyzed with appropriate time lags in simple models (Descloux *et al.*, 2012; Sang *et al.*, 2015). At a national scale, the disease exhibits seasonal waves and regional synchronies that help position the Western Amazon within coherent risk calendars (Churakov *et al.*, 2019). Simultaneously, citizen science initiatives increase the reach and speed of detection, with the GLOBE Observer Mosquito Habitat Mapper

(MHM) protocol generating georeferenced data useful for education and participatory surveillance (Low et al., 2021; Carney et al., 2022).

The practical significance is direct: combining reliable meteorological data from the National Institute of Meteorology (INMET) and the National Aeronautics and Space Administration (NASA) Earth System Data Explorer with citizen-led MHM observations can produce a local indicator for timely interventions, risk communication, and educational actions (INMET, 2025; NASA, 2025a). This integration mobilizes schools, health agents, and residents as co-producers of evidence and immediate intervention, leading to the research question of this study: Given the high incidence of dengue in Ji-Paraná, how does the variation in atmospheric conditions (temperature and precipitation) correlate with larval infestation observed by the Mosquito Habitat Mapper (MHM) Protocol—Hydrosphere component—across different neighborhoods, and what is the predictive potential of these data for arbovirus surveillance?

The study is based on two hypotheses: (H1) active mapping and sampling will reveal the concentration of Aedes genus larvae at multiple points throughout the city; (H2) there will be a positive correlation between locations with higher larval infestation and favorable atmospheric conditions (temperature and precipitation), indicating ideal bioclimatic conditions and predictive potential usable by surveillance systems.

2. Introduction

Dengue remains a growing challenge in Brazil, presenting seasonal patterns and regional synchronies that help position the Western Amazon within high-risk windows (Churakov et al., 2019). In Rondônia, documented increases in incidence and social costs associated with the disease reinforce the need for evidence-based strategies with a territorial focus (Abe & Miraglia, 2018). In 2025, Ji-Paraná recorded an alert for the reintroduction of the dengue virus serotype 3 (DENV-3) and reports of high Aedes aegypti infestation in city areas, putting pressure on local surveillance and the demand for simple, transparent, and actionable metrics (Goulart et al., 2024; Nogueira, 2025; Pessoa, 2025b).

From a scientific perspective, atmospheric variables such as temperature and precipitation modulate critical stages of dengue's eco-epidemiology and can support predictions when treated with appropriate time lags (Descloux et al., 2012; Sang et al., 2015). Concurrently, citizen science initiatives increase the reach and speed of breeding site detection, with the Mosquito Habitat Mapper (MHM) protocol established as an educational and participatory surveillance tool, generating georeferenced records of breeding sites and immature stages of the vector (Carney et al., 2022; Low et al., 2021). This convergence allows the topic to be framed under the Earth as a System approach, connecting the Hydrosphere—observed by the MHM—to the Atmosphere, described by standardized meteorological series.

The gap this study addresses is the scarcity of local, reproducible, and low-cost arrangements that systematically integrate citizen science data on larval infestation with official atmospheric information to produce a useful indicator for municipal decision-making. The purpose is to examine the relationship between atmospheric conditions and signs of larval infestation in neighborhoods of Ji-Paraná and to evaluate the potential of these inputs to support surveillance, articulating scientific evidence and community action.

Operationally, the work integrates data from the National Institute of Meteorology (INMET) and the National Aeronautics and Space Administration (NASA) – Earth System Data Explorer with georeferenced records from the Mosquito Habitat Mapper (MHM) protocol to inform a local risk indicator and its applications in health communication and response (INMET, 2025; NASA, 2025a).

3. Theoretical Framework

This section presents the theoretical framework supporting the study, articulating three axes: (i) the recent epidemiological scenario in Ji-Paraná and its risk factors; (ii) the

bioclimatology of *Aedes aegypti* and its relationships with temperature and precipitation; and (iii) the principles of predictive surveillance anchored in the Mosquito Habitat Mapper (MHM) protocol under the Earth System approach, connecting the Hydrosphere and Atmosphere. Together, these axes synthesize evidence on seasonal waves and regional synchronies that inform risk windows (Churakov et al., 2019), on how atmospheric variables modulate vector dynamics and allow for risk anticipation when treated with appropriate time lags (Descloux et al., 2012; Sang et al., 2015), and on the role of citizen science in generating georeferenced data useful for decision-making through the MHM (Carney et al., 2022; Low et al., 2021).

3.1 Dengue in Ji-Paraná: Epidemiological Scenario and Risk Factors

In Ji-Paraná, Nogueira (2025) describes the alert for the reintroduction of DENV-3, while Pessoa (2025b) reports high levels of Aedes aegypti infestation in urban areas. Taken together, these sources outline an expanded risk framework that manifests heterogeneously across the territory, as observed by Goulart and colleagues when analyzing the recent distribution of the disease in the municipality (Goulart et al., 2024).

At the scale of local planning, this epidemiological mosaic reinforces the need for simple metrics that convert environmental signals and field observations into timely decisions. This guideline converges with participatory and integrated surveillance proposals discussed by Carney and co-authors and with the operational utility of the Mosquito Habitat Mapper protocol for detecting breeding sites and immature stages (Carney et al., 2022; Low et al., 2021).

Abe and Miraglia (2018) show that phases of urban transformation in Rondônia were associated with increases in cases and costs, which recovers the socioeconomic dimension of the problem. When this history is placed alongside the regionally propagating seasonal waves described by Churakov et al. (2019), the municipality gains a basis to align short-term actions with the broader climate calendar and reduce social and operational costs through an indicator anchored in local evidence.

Additionally, the municipality presents an adaptive capacity index of 0.48 (medium level) for arboviruses on the AdaptaBrasil platform (2025), defined as the socio-ecological system's ability to prepare for and adjust to climate threats. This data is used for contextualization only, without being integrated into the analyses.

3.2 The Aedes aegypti Mosquito and Bioclimatology

On the bioclimatic level, Descloux et al. (2012) show that temperature and precipitation modulate essential stages of the vector cycle and transmission, and that these relationships become informative when analyzed with time lags consistent with Aedes biology. Sang and colleagues reach convergent conclusions by demonstrating predictive gains in models that incorporate atmospheric variables and appropriate time windows (Sang et al., 2015).

To situate Ji-Paraná in time and space, Churakov et al. (2019) describe national seasonal synchronies, while Varamballi and colleagues highlight that climate suitability for Aedes is highly heterogeneous. Gui et al. (2021) remind us that responses to atmospheric conditions can be complex in the short term, which justifies opting for direct and granular measures of infestation via the Mosquito Habitat Mapper protocol, as argued by citizen science initiatives oriented toward participatory surveillance (Low et al., 2021; Varamballi et al., 2024).

3.3 Predictive Surveillance and the MHM Protocol (Hydrosphere)

From a surveillance perspective, Low and colleagues document that the Mosquito Habitat Mapper protocol produces georeferenced records of breeding sites and immature stages useful for education and local decision-making. In parallel, Carney et al. (2022) advocate for the integration of citizen science platforms as the basis for next-generation surveillance, which is

more capillary and rapid than exclusively official arrangements, provided that participation biases are monitored (Low et al., 2021).

To ensure comparability and reproducibility, Hydrosphere observations obtained by the MHM must be paired with Atmosphere series from official sources. The National Institute of Meteorology (INMET) provides an operational reference at the local scale, while NASA's Earth System Data Explorer provides environmental variables with consistent spatial coverage. This composition is aligned with the Earth System approach and guides the temporal and spatial harmonization of data, including the careful exploration of time lags (INMET, 2025; NASA, 2025a).

It is at this junction that the present study is positioned; by integrating early signals in the Hydrosphere measured by the MHM with official atmospheric series from INMET and NASA, priority is given to a simple, transparent, and actionable indicator based on correlation with time lags. Applied climate literature suggests that this foundation offers immediate utility to municipal management and may, in the future, support analytical extensions without shifting focus away from parsimonious and high-operational-value solutions (Conde-Gutiérrez et al., 2024; Descloux et al., 2012; Sang et al., 2015).

4. Trap Construction and Monitoring

The study was conducted in Ji-Paraná (RO). According to the IBGE (2024), the municipality has 53 neighborhoods and two districts. The study took place between September 7 and October 11, 2025 (five consecutive weeks), with data consolidated into epidemiological weeks (Sunday–Saturday). To spatially situate the sampling, the urban study area is presented in Figure 1.

Nine sampling points were defined in neighborhoods with environmental and urban heterogeneity (shading, soil permeability, proximity to vegetation/watercourses, safety, and access). Each point received a trap, and the official list of locations, including the neighborhood and microenvironment description, is found in Table 1.

Figure 1
Map of trap distribution

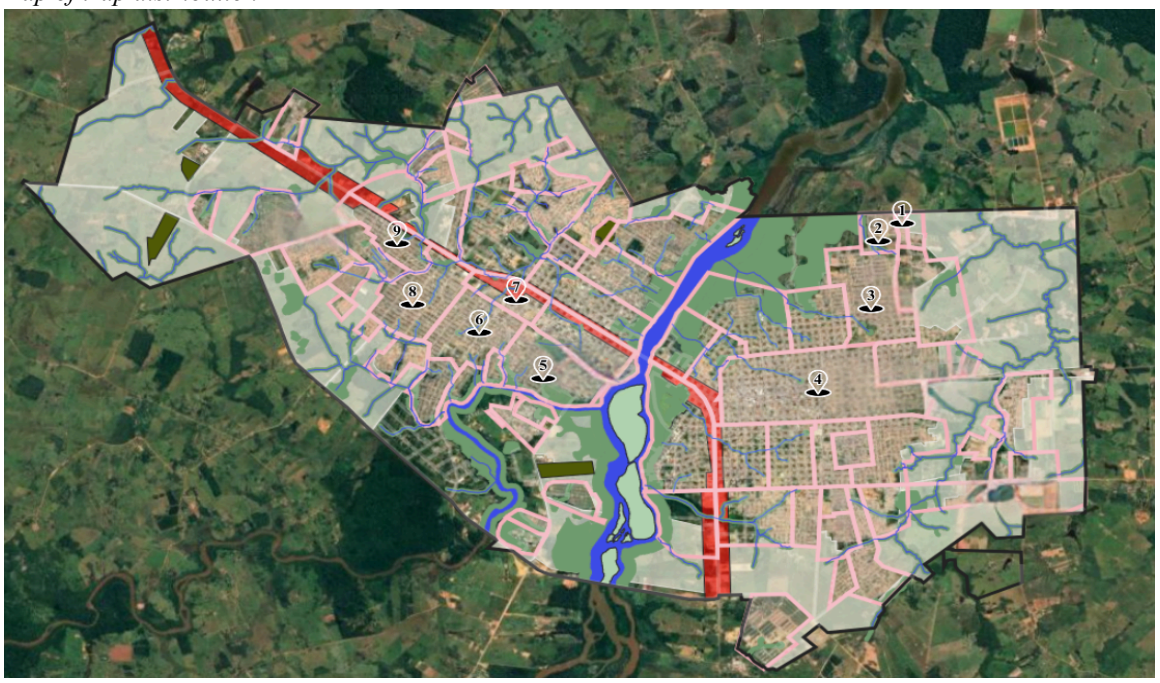

Note. Prepared by the authors using Google Maps (2025).

Table 1

Detailed description of the environment

PONTO	BAIRRO	DESCRIÇÃO
1	Residencial Carneiro	Predominantly artificial peridomiciliary environment, characterized by high anthropic intervention, high walls, and a mostly cemented yard. A residual area of soil (sand and gravel) features ground vegetation and a fruit tree (*Malpighia emarginata* / Acerola). The arboreal vegetation creates specific shading points, contrasting with the paved surface.
2	Boa Esperança	Environment classified as a vacant lot, with high density of secondary and/or ground vegetation. The absence of residential intervention and direct exposure to the natural environment suggests earth soil and high humidity, especially after rainfall. This site shows characteristics of neglect or unstructured use, which may lead to the accumulation of debris.
3	JK	Peridomiciliary yard area with high vegetation density and presence of crops. The environment has exposed soil and is dominated by dense leaf cover that provides intense shade and contributes to moisture retention in the substrate.
4	Nova Brasília	Structurally protected peridomiciliary environment, characterized by a shaded corner with masonry walls and ceramic flooring. The area shows an accumulation of plant debris on the substrate.
5	Urupá	Located in a peridomiciliary yard area with low topography; the most relevant factor is the presence of a stream (natural watercourse). The surroundings are dominated by high and dense vegetation (secondary forest/Permanent Preservation Area - APP), creating a thick canopy and intense shade. The hydrography and vegetation are factors of environmental stability.
6	Jardim dos Migrantes	Residential peridomiciliary environment with a fully cemented (paved) yard, indicating a high level of human intervention. The only vegetation present is a small gardening area (flowers). The cement reduces the potential for soil moisture.
7	2 de Abril	Located in an office environment with high anthropic intervention, featuring a fully cemented (paved) yard. Vegetation is restricted to small gardening areas (flowers) in the front. The environment is predominantly dry and artificial.
8	Jardim Presidencial	Peridomiciliary environment with high walls and predominant cemented paving. The only area without cement is covered with fine gravel, a substrate that maximizes drainage and prevents soil moisture retention. There is no significant arboreal or shrubby vegetation.
9	Santiago	Peridomiciliary yard area with high density of shrubby vegetation and crops. The environment has earth soil and grass, featuring an accumulation of dry biomass near the side structures (walls). The dense vegetation cover is the dominant factor, creating multiple shaded and humid microclimates.

Note. Prepared by the authors (2025).

The traps were made using 2L PET bottles, micro-mesh (tule), seal rings, sandpaper, electrical tape, and simple bait (e.g., fish food), following a standardized sequence: funnel cutting, internal sanding, mesh fixation, and water level adjustment a few centimeters below the neck (**Figure 2**).

Figure 2

Armadilhas passo a passo e confeccionadas

Nota. Adapted from NASA (2025b; 2025c).

The monitoring was weekly during the five weeks, keeping one active trap per point each week. In each reading, date/time, coordinates, presence/absence of immatures, counts of larvae and pupae, observations (e.g.: drying, tipping) and local action when pertinent were recorded. The data were noted in standardized field sheets (**Figure 3.a**) and subsequently inserted into the Mosquito Habitat Mapper (MHM) protocol via the GLOBE Observer app (**Figure 3.b**), with a double consistency check (dates/hours, location and photos), according to good practices of citizen science (Carney et al., 2022; Low et al., 2021).

Figura 3
(a) Field sheets and (b) GLOBE Observer app

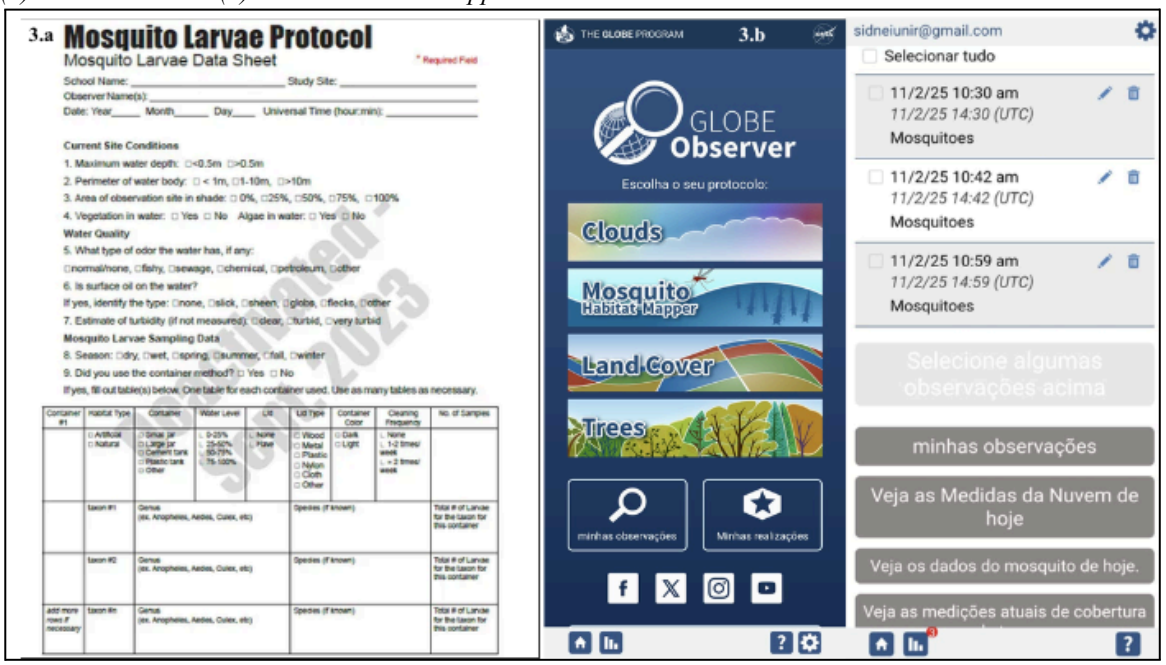

Note. Adapted from NASA (2025b; 2025c).

The atmospheric variables — minimum, average and maximum temperature (°C) and precipitation (mm) — were obtained from INMET and My NASA Data in daily resolution, with weekly aggregation and alignment to the epidemiological weeks of the Hydrosphere component (INMET, 2025; NASA, 2025a). The relationship between the weekly MHM indicators (e.g.: total larvae and positivity) and the climate variables (e.g.: weekly precipitation and weekly average temperature) was estimated by Pearson correlation.

5. Results

5.1 Breeding Site Mapping and Larval Distribution

The larval monitoring performed during five consecutive weeks resulted in the detection of 86 Aedes aegypti larvae distributed across the nine sampling points. The temporal distribution presented significant variation, with Week 2 recording the largest number of larvae (24 specimens, 48.8% of the total), followed by Week 4 (29 larvae, 33.7%), Week 3 (9 larvae, 10.5%), Week 5 (3 larvae, 3.5%) and Week 1 (3 larvae, 3.5%). The average of larvae per trap varied from 0.33 (Weeks 1 and 5) to 4.67 (Week 2), evidencing a sharp temporal amplitude in the detection of immature forms.

The spatial distribution revealed heterogeneity between the sampling points, with three locations concentrating 69.8% of the larvae detected: Urupá (23 larvae, 26.7%), Boa Esperança

(21 larvae, 24.4%) and JK (16 larvae, 18.6%). The other points presented reduced detection, with Nova Brasília and Santiago recording 12 larvae each (14.0%), and Residencial Carneiro, Jardim dos Migrantes, 2 de Abril and Jardim Presidencial presenting 3 larvae each (3.5%). Four points did not present detection in three or more weeks of the monitored period, while Urupá was the only point with a positive record in all five consecutive weeks.

Table 1 presents the complete distribution of larval records by sampling point and monitoring week, evidencing the spatio-temporal variability of the infestation in the municipality during the study period.

Table 1
Weekly record of Aedes aegypti larvae by sampling point

POINT - NEIGHBORHOOD	WEEKS					TOTAL
	1	*2*	*3*	*4*	*5*	
1 - Residencial Carneiro	0	0	1	2	0	**3**
2 - Boa Esperança	1	12	5	2	1	**21**
3 - JK	0	2	4	3	2	**11**
4 - Nova Brasília	0	1	3	1	2	**7**
5 - Urupá	2	4	9	5	3	**23**
6 - Jardim dos Migrantes	0	0	1	1	1	**3**
7 - 2 de Abril	0	1	1	1	0	**3**
8 - Jardim Presidencial	0	1	1	0	1	**3**
9 - Santiago	0	3	4	2	3	**12**
Weekly Total	**3**	**24**	**29**	**17**	**13**	**86**

Note. Prepared by the authors (2025).

5.2 Bioclimatic Correlation Results

The climatological monitoring recorded 89.09 mm of accumulated precipitation in Ji-Paraná, distributed irregularly over the five weeks of collection. Week 3 concentrated the largest rainfall volume (37.20 mm), representing 41.8% of the total accumulated in the period, while Week 5 recorded only 2.43 mm, the lowest index observed. The daily average precipitation varied from 0.35 mm (Week 5) to 5.31 mm (Week 3). The most intense precipitation event occurred on September 23, with a record of 21.48 mm in 24 hours, followed by 12.63 mm on September 24.

The maximum temperatures presented an amplitude of 8.10°C throughout the period, with a record of 39.10°C on September 12 and 31.00°C on October 02. The weekly average of maximum temperatures varied between 34.37°C (Week 4) and 37.53°C (Week 1). The average temperatures fluctuated between 26.77°C (Week 4) and 29.18°C (Week 1), with an amplitude of 2.41°C. The minimum temperatures recorded a minimum value of 20.00°C on September 07 and a maximum of 24.50°C on September 10, with weekly averages varying between 22.36°C and 23.23°C.

The temporal distribution of precipitation presented the following weekly totals: Week 1 with 10.56 mm, Week 2 with 15.57 mm, Week 3 with 37.20 mm, Week 4 with 24.33 mm and Week 5 with 2.43 mm. Week 1 presented two main precipitation events on September 10 and 13 (5.22 mm and 4.43 mm, respectively). Week 2 recorded five days with the occurrence of rain, with September 18 being the rainiest day (6.60 mm). Week 3 concentrated the precipitation on September 23 and 24, with 21.48 mm and 12.63 mm. Week 4 recorded two main peaks on September 28 and 30 (9.62 mm and 10.31 mm). Week 5 presented minimum accumulated precipitation, with only one significant event on October 10 (1.60 mm).

Table 2 presents the weekly averages of the climatological parameters, while Figure 4 details the daily variation of precipitation and temperatures throughout the monitoring period.

Table 2

Weekly averages of the recorded climatological parameters

WEEK (*Period*))	PRECIPITATION (MM)		TEMPERATURE (°C)		
	Daily Average	*Weekly Total*	*Average Maximum*	*Average*	*Average Minimum*
1 (07/09 - 13/09)	1,51	10,56	37,53	29,18	22,93
2 (14/09 - 20/09)	2,22	15,57	35,53	27,56	23,23
3 (21/09 - 27/09)	5,31	37,2	34,91	27,48	22,74
4 (28/09 - 04/10)	3,48	24,33	34,37	26,77	22,36
5 (05/10 - 11/10)	0,35	2,43	34,79	27,87	22,93
Total/Average of the Period	**2,54**	**89,09**	**35,43**	**27,77**	**22,84**

Note. Adapted from INMET (2025) and NASA (2025a).

Figure 4

Graph of daily temporal variation of climatic variables during the research period

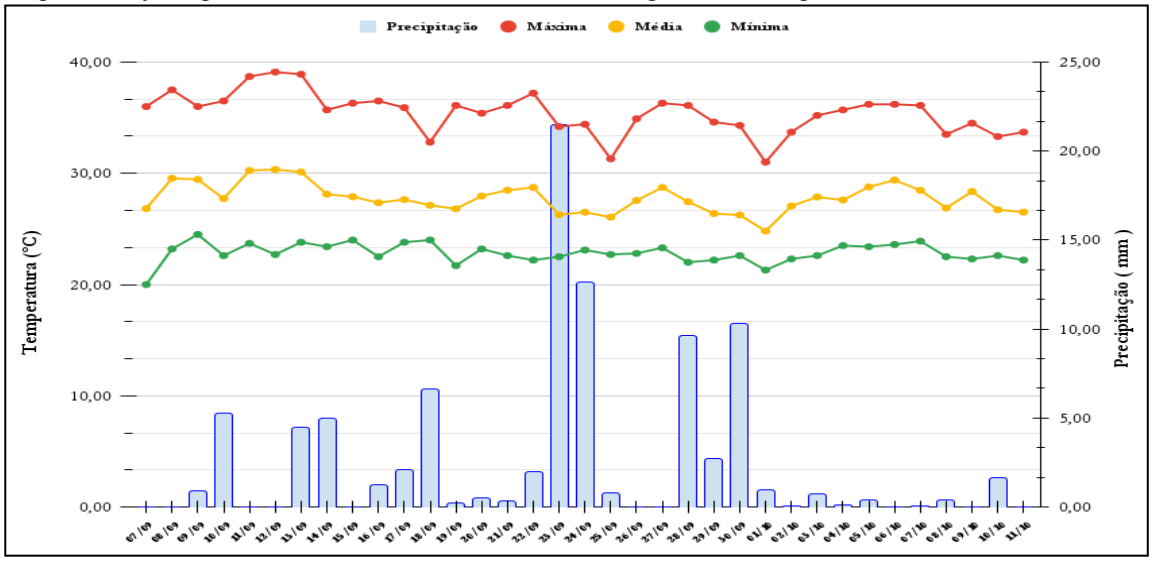

Note. Adapted from INMET (2025) and NASA (2025a).

5.3 Relationship Between Atmospheric Conditions and Aedes aegypti Larval Density

With n = 5 weeks, the correlations must be read as exploratory. At lag 0, r = +0.52 was observed between weekly precipitation and larvae (moderate positive association) and r = -0.63 between weekly average temperature and larvae (moderate negative association).

The weekly distribution of values supports these signs. Week 3 concentrated the largest volume of rain (37.20 mm; 41.8% of the total) and the peak of larvae (29; 33.7% of the total). Week 4 recorded 24.33 mm and 17 larvae; together, Weeks 3–4 sum 69.1% of the rain for the period and 53.5% of the larvae (46/86). In contrast, Week 5, with 2.43 mm (2.7% of the total), had 13 larvae; and Week 1, with 10.56 mm, recorded 3 larvae.

As for temperature, the warmest week was Week 1 (29.18 °C) with 3 larvae, while Week 3 presented 27.48 °C and 29 larvae. Week 4 had the lowest average (26.77 °C) and 17 larvae. The thermal amplitude in the period was 2.41 °C (26.77–29.18 °C), with a slightly descending trajectory until Week 4 and a discrete elevation in Week 5 (27.87 °C), accompanied by 13 larvae.

Figure 5 integrates the three series and evidences: (i) concomitant peak of rain and larvae in Week 3; (ii) reduction of larvae in the weeks of low rain; and (iii) inverse relationship with the average temperature in the observed interval.

Figure 5

Temporal variation of larval density and atmospheric conditions during the monitoring period

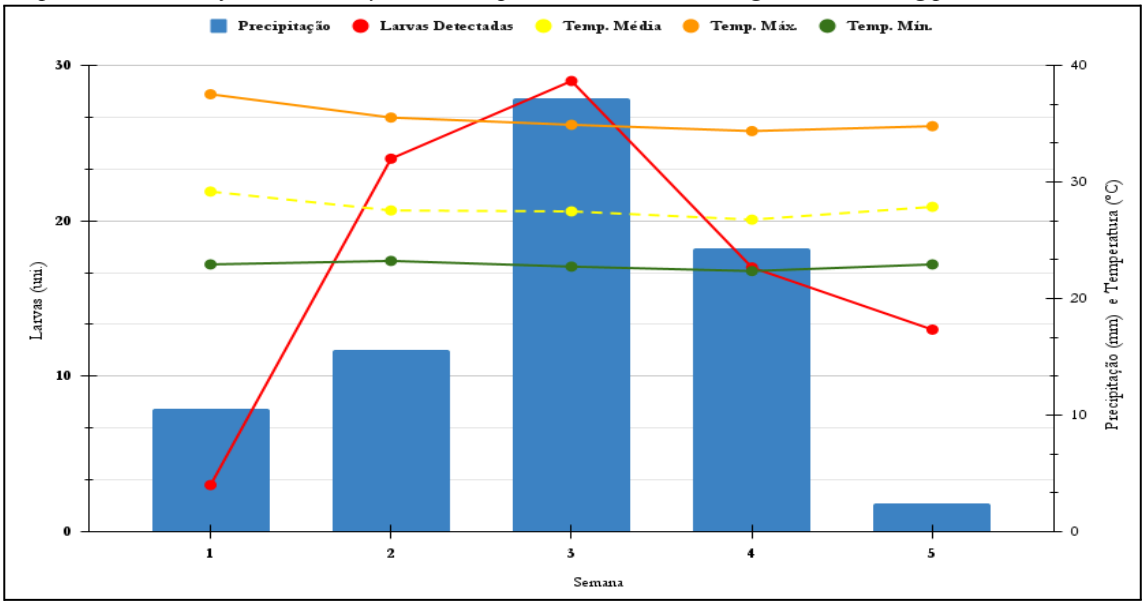

Note. Adapted from INMET (2025) and NASA (2025a; 2025b; 2025c).

6. Discussion

The results show unequal distribution of larval infestation over the weeks and among neighborhoods, with concentrated peaks and persistence in at least one point. This picture is consistent with local evidence of territorial foci and seasonality, reinforcing the necessity of prioritization of areas in the municipal response given the return of DENV-3 (Goulart et al., 2024; Nogueira, 2025; Pessoa, 2025b).

In the climatic axis, a moderate positive association was observed between weekly rain and larvae ($r = 0.52$). This pattern is compatible with the creation of containers and accumulation of water after moderate rainfall pulses; at the same time, the literature warns that very intense rains can exert a "flushing" effect depending on the analyzed lag, which guides timely blockages immediately after precipitation peaks and the testing of accumulated windows in future analyses (Descloux et al., 2012; Gui et al., 2021; Sang et al., 2015).

The moderate negative association between average temperature and larvae ($r = -0.63$) suggests that, in the observed interval (≈26.8–29.2 °C), slightly less warm weeks favored detection. This is coherent with a narrow thermal optimum for vector and virus described in tropical contexts: gains up to ~28 °C and attenuation above that (Descloux et al., 2012; Gui et al., 2021). At a national scale, seasonal waves that advance from West to East help to anchor the local operational calendar (Churakov et al., 2019).

Operationally, georeferenced and replicable records via the Mosquito Habitat Mapper (MHM) protocol, combined with INMET/NASA series, allow for the composition of a simple weekly indicator (larvae/positivity × accumulated rain in 1–2 weeks × average temperature) to trigger actions: intensify blockages, direct risk communication and educational actions in priority neighborhoods (Carney et al., 2022; Low et al., 2021).

Taken together, the results confirm H1 – there was infestation in multiple points, with persistence in at least one neighborhood – and partially corroborate H2: rain was positively associated with larvae, while temperature, at lag 0, showed a negative association, plausible in a window close to the thermal optimum. The short duration (five weeks), one trap per point and the absence of formal lags may have masked late effects; therefore, we suggest expanding the period, testing lags (1–3) and accumulated rain, modeling non-linearities and reinforcing the sampling

per neighborhood. Operationally, this supports post-rain blockages and risk communication in thermally favorable windows.

7. Conclusion

This study integrated local observations of the Mosquito Habitat Mapper (MHM) protocol with official atmospheric series (INMET/NASA) to examine the relationship between climate and larval infestation signs in Ji-Paraná. We found unequal distribution in space and time, with concentrated peaks and persistence in at least one sampling point. In statistical terms, a moderate positive association between weekly rain and larvae and a moderate negative association with the average temperature at lag 0 were observed. Thus, H1 was confirmed, while H2 was partially confirmed: the rainfall component aligned with expectations, while temperature showed an inverse signal in the short term, plausible in a window close to the thermal optimum and under a short series.

From a scientific point of view, the main contribution is to demonstrate the feasibility of a simple, transparent, and replicable indicator, resulting from the pairing between citizen data (MHM) and official meteorological data. This architecture, coherent with the Earth as a System approach, offers a parsimonious path to generate local alert signals from weekly measurements, with potential for generalization to other Amazonian schools and municipalities. By anchoring surveillance in low-cost data, the work advances local eco-epidemiological understanding and establishes a baseline for future predictive modules.

The practical implications are direct: a weekly dashboard (larvae/positivity × accumulated rain with lag × average temperature) can guide timely blockages after precipitation pulses, risk communication in thermally favorable windows, and educational actions focused on priority neighborhoods. In a scenario of the return of DENV-3, incorporating this dashboard into the routine cycle of surveillance and health education allows for territorial prioritization, pre-positioning of inputs, and efficient use of teams, reinforcing local response capacity.

As next steps, it is recommended to expand the series to 12–16 weeks, increase the sampling density (more traps per neighborhood), test lags (1–3 weeks) and moving windows of rain, and explore non-linearities (e.g., DLNM/Poisson), as well as record possible confounders (microclimate, household storage, control actions). Complementary GLOBE protocols can enrich the model – notably Land Cover to characterize microenvironments and Surface Temperature to assess local thermal variations – in addition to low-cost rain gauges for field validation.

The mentor guidance was decisive for standardizing the collection, ensuring quality and safety, and aligning the analysis with the expected methodological rigor, consolidating a reproducible and scalable arrangement for the school network and municipal management.

References

Abe, K. C., & Miraglia, S. G. E. K. (2018). Dengue incidence and associated costs in the periods before (2000-2008) and after (2009-2013) the construction of the hydroelectric power plants in Rondônia, Brazil. *Epidemiologia e Servicos de Saude: Revista Do Sistema Unico de Saude Do Brasil*, *27*(2), e2017232.

Carney, R. M., Mapes, C., Low, R. D., Long, A., Bowser, A., Durieux, D., Rivera, K., Dekramanjian, B., Bartumeus, F., Guerrero, D., Seltzer, C. E., Azam, F., Chellappan, S., & Palmer, J. R. B. (2022). Integrating global citizen science platforms to enable next-generation surveillance of invasive and vector mosquitoes. *Insects*, *13*(8), 675.

Churakov, M., Villabona-Arenas, C. J., Kraemer, M. U. G., Salje, H., & Cauchemez, S. (2019). Spatio-temporal dynamics of dengue in Brazil: Seasonal travelling waves and determinants of regional synchrony. *PLoS Neglected Tropical Diseases*, *13*(4), e0007012.

Conde-Gutiérrez, R. A., Colorado, D., Márquez-Nolasco, A., & Gonzalez-Flores, P. B. (2024). Parallel prediction of dengue cases with different risks in Mexico using an artificial neural network model considering meteorological data. *International Journal of Biometeorology*, *68*(6), 1043–1060.

Descloux, E., Mangeas, M., Menkes, C. E., Lengaigne, M., Leroy, A., Tehei, T., Guillaumot, L., Teurlai, M., Gourinat, A.-C., Benzler, J., Pfannstiel, A., Grangeon, J.-P., Degallier, N., & De Lamballerie, X. (2012). Climate-based models for understanding and forecasting dengue epidemics. *PLoS Neglected Tropical Diseases*, *6*(2), e1470.

Goulart, F. O., Carbonera, G. B. O., Turatti, M. E. R., Faust, M. B., Somenzari, N., Miranda, A. M., & Silva, F. C. (2024). Análise sobre a incidência de dengue no município de Ji-Paraná nos últimos três anos. Em *Anais do 9º Fórum Rondoniense de Pesquisa*, 4.

Gui, H., Gwee, S., Koh, J., & Pang, J. (2021). Weather factors associated with reduced risk of dengue transmission in an urbanized tropical city. *International Journal of Environmental Research and Public Health*, *19*(1), 339.

Instituto Brasileiro de Geografia e Estatística (IBGE). (2023). *Panorama: Ji-Paraná*. https://cidades.ibge.gov.br/brasil/ro/ji-parana/panorama

Instituto Nacional de Meteorologia - INMET. (2025). *Dados Históricos*. Gov.br. https://portal.inmet.gov.br/

Low, R., Boger, R., Nelson, P., & Kimura, M. (2021). GLOBE Mosquito Habitat Mapper citizen science data 2017-2020. *GeoHealth*, *5*(10), e2021GH000436.

Low, R. D., Schwerin, T. G., Boger, R. A., Soeffing, C., Nelson, P. V., Bartlett, D., Ingle, P., Kimura, M., & Clark, A. (2022). Building international capacity for citizen scientist engagement in mosquito surveillance and mitigation: The GLOB[1]E Program's GLOBE Observer Mosquito Habitat Mapper. *Insects*, *13*(7), 624.

Ministério da Ciência, Tecnologia e Inovações (MCTI). (2025). *AdaptaBrasil MCTI: Dados e impactos*. https://sistema.adaptabrasil.mcti.gov.br/

National Aeronautics and Space Administration (NASA). (2025a). *Earth system data explorer*. My NASA Data - Earthengine.App. https://larc-mynasadata-2df7cce0.projects.earthengine.app/view/earth-system-data-explorer

National Aeronautics and Space Administration (NASA). (2025b). *GLOBE observer*. GLOBE Observer - Globe.gov. https://observer.globe.gov/

National Aeronautics and Space Administration (NASA). (2025c). *GLOBE Program*. Globe.gov. https://www.globe.gov/

Nogueira, J. (2025, outubro 20). *Secretaria confirma casos de Dengue Tipo 3 no município - Uma ação de prevenção deverá chegar em todos os bairros da cidade*. Portal Sistema Gurgacz de Comunicão. https://sgc.com.br/noticia/6/430915/secretaria-confirma-casos-de-dengue-tipo-3-no- municipio

Pessoa, N. (2025, março). *Relatório aponta bairros com maior índice de infestação do Aedes aegypti em Ji-Paraná*. Prefeitura de Ji-Paraná. https://ji-parana.ro.gov.br/noticias/relatorio-aponta-bairros-com-maior-indice-de-infestacao-do-aedes-aeg ypti-em-ji-p arana/

Pessoa, N. (2025, outubro). *Prefeitura de Ji-Paraná alerta para retorno do sorotipo 3 da dengue e reforça ações de combate*. Prefeitura de Ji-Paraná. https://ji-parana.ro.gov.br/noticias/prefeitura-de-ji-parana-alerta-para-retorno-do-sorotipo-3-da-dengue-e-reforca-acoes-de-combate/

Sang, S., Gu, S., Bi, P., Yang, W., Yang, Z., Xu, L., Yang, J., Liu, X., Jiang, T., Wu, H., Chu, C., & Liu, Q. (2015). Predicting unprecedented dengue outbreak using imported cases and climatic factors in Guangzhou, 2014. *PLoS Neglected Tropical Diseases*, *9*(5), e0003808.

Varamballi, P., Babu N, N., Mudgal, P. P., Shetty, U., Jayaram, A., Karunakaran, K., Arumugam, S., & Mukhopadhyay, C. (2024). Spatial heterogeneity in the potential distribution of Aedes mosquitoes in India under current and future climatic scenarios. *Acta Tropica*, *260*(107403), 107403.